

Organometallic-mediated radical polymerization using well-defined Schiff base cobalt(II) complexes

Yan F. Silva, Beatriz A. Riga, Victor M. Deflon, Jhonathan R. Souza, Leonardo H. F. Silva, Antonio E. H. Machado, Pedro Ivo S. Maia, Valdemiro P. Carvalho-Jr & Beatriz E. Goi

To cite this article: Yan F. Silva, Beatriz A. Riga, Victor M. Deflon, Jhonathan R. Souza, Leonardo H. F. Silva, Antonio E. H. Machado, Pedro Ivo S. Maia, Valdemiro P. Carvalho-Jr & Beatriz E. Goi (2018): Organometallic-mediated radical polymerization using well-defined Schiff base cobalt(II) complexes, Journal of Coordination Chemistry, DOI: [10.1080/00958972.2018.1527322](https://doi.org/10.1080/00958972.2018.1527322)

To link to this article: <https://doi.org/10.1080/00958972.2018.1527322>

 View supplementary material 

 Accepted author version posted online: 22 Sep 2018.

 Submit your article to this journal 

 View Crossmark data 

Organometallic-mediated radical polymerization using well-defined Schiff base cobalt(II) complexes

YAN F. SILVA^a, BEATRIZ A. RIGA^a, VICTOR M. DEFLON^b, JHONATHAN R. SOUZA^c,
LEONARDO H. F. SILVA^c, ANTONIO E. H. MACHADO^c, PEDRO IVO S. MAIA^d,
VALDEMIRO P. CARVALHO-JR^a and BEATRIZ E. GOI^{*a}

^aFaculdade de Ciências e Tecnologia, UNESP – Univ. Estadual Paulista, CEP 19060-900,
Presidente Prudente, SP, Brazil

^bInstituto de Química de São Carlos, Universidade de São Paulo, CEP 13560-970, São Carlos, SP, Brazil

^cInstituto de Química, Universidade Federal de Uberlândia, P.O. Box 593, Uberlândia 38400-089,
Minas Gerais, Brazil

^dDepartamento de Química, Universidade Federal do Triângulo Mineiro, CEP 38025-440, Uberaba, MG, Brazil

A series of new cobalt(II) complexes of Schiff base derived from salicylaldehyde and different cycloalkylamines (cycloalkyl = cyclopentyl-**1a**, cyclohexyl-**1b**, and cycloheptyl-**1c**) was synthesized: [Co(CyPen-Salicyl)₂] (**2a**), [Co(CyHex-Salicyl)₂] (**2b**), and [Co(CyHep-Salicyl)₂] (**2c**). The bis(phenoxyiminato)Co(II) complexes (**2a-2c**) have been fully characterized by FTIR and UV-Vis spectroscopy, elemental analysis, cyclic voltammetry, computational methods, and two of the complexes were further studied by single crystal X-ray crystallography. The X-ray structure analysis of **2a-b** shows that the geometry around the metal atom is a distorted tetrahedron, confirming the spectroscopic data. Electrochemical studies suggest that the redox potential of **2a-2c** are sensitive to the substituent group, decreasing in order cyclopentyl > cyclohexyl > cycloheptyl. Complexes **2a-2c** were used as controlling agents for the polymerization of vinyl acetate (VAc) initiated by AIBN, according to a cobalt-mediated radical polymerization (CMRP) mechanism. The VAc polymerization mediated by **2a-2c** suggests that the level of control can be slightly tuned by the substitution of the cycloalkyl group on the Schiff base ligand. Complex **2b** showed the smaller discrepancy between observed and calculated molecular weight, and narrower molecular weight distribution.

Keywords: Schiff base; Cobalt(II) complexes; Polymerization; Vinyl acetate; CMRP

*Corresponding author. Email: beatriz_goi@fct.unesp.br

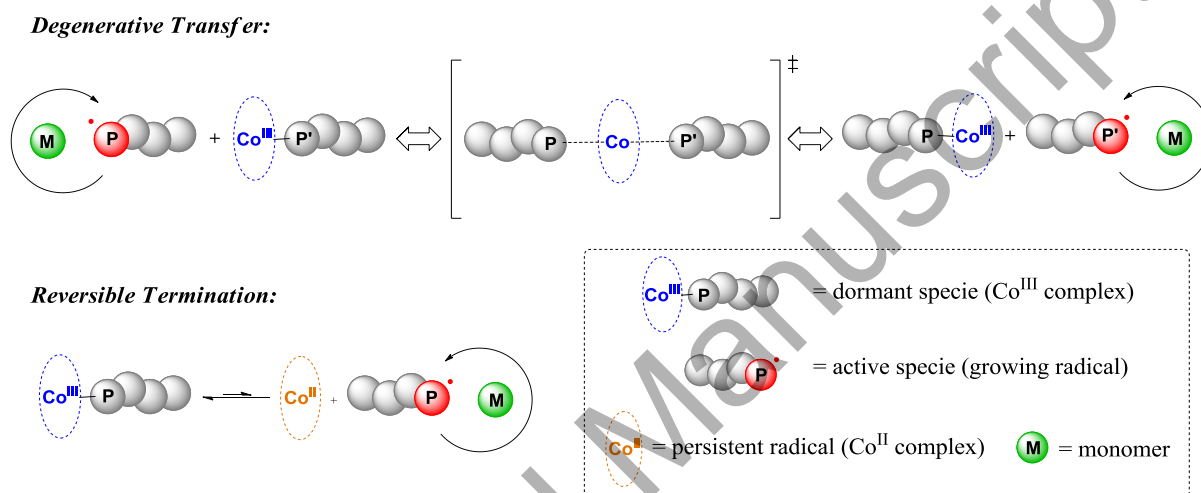
1. Introduction

Schiff bases play an important role in inorganic chemistry as they can easily form stable complexes with most transition metal ions. This superabundant interest comes from the numerous and various applications of Schiff base metal complexes. Schiff bases and their metal complexes have large potential applications in various fields including optical [1-5], magnetic [6] and supramolecular materials [7-9] as well as chemical probes [10, 11] and catalysis [4, 12-15].

Schiff base complexes have been used as highly efficient catalysts for cyclopropanation, oxidation, epoxidation, Diels-Alder, and polymerization reactions [4, 12-21]. In particular, Schiff base cobalt complexes are an interesting class of compounds for mediating the polymerization of polar monomers including VAc (vinyl acetate) due to their less oxophilic nature relative to early transition metals. This monomer can be polymerized exclusively via a radical mechanism [22], so its “living” polymerization may only be considered using modern “living”/controlled radical polymerization (CRP) methodologies based on the reversible equilibrium between growing radicals and dormant species [23-27]. N₂O₂ Schiff base cobalt-mediated radical polymerization has been extended to VAc [28-30]. In a recent report, Peng and coworkers described the cobalt-mediated radical polymerization (CMRP) of both vinyl acetate and methyl acrylate using a Schiff base cobalt complex as controlling agent [29]. They reported a good control over the two polymerizations with the formation of polymers with low dispersities. Debuigne and coworkers replace the bidentate acac ligand for a tetradentate Salen type ligand in a one-pot process for improving the block copolymerization of vinyl acetate and *n*-butyl acrylate [31].

It is well known that CMRP, while technically belonging to the organometallic-mediated radical polymerization (OMRP) class, has interesting advantages such as enabling the synthesis of complex architecture polymers [32-36] and the obtention of polymers with well-defined properties [29, 36-39]. Moreover, it is by far the most efficient technique to synthesize controlled polymers of VAc, which is a less activated monomer (LAM) capable of generating more reactive radicals [38, 40-42]. The success of this technique is mostly attributed to its mechanism and the reversible formation of a Co-carbon covalent bond. This reactional mechanism is based on a temporary reversible deactivation of the growing radicals, which coordinate to the metal center to reduce the instant concentrations of radicals, minimizing the possibility of irreversible terminations to occur [43]. Depending on the source and concentration of radicals, the

mechanism follows two different pathways, degenerative transfer (DT) or reversible termination (RT) [44-46]. In the former case, the radical source is exclusively the initiator, and the radical concentration is determined by the initiator concentration. Contrarily, in the RT pathway the radical species enter the reaction dissociated from the organo-cobalt complex ($\text{Co}^{\text{III}}\text{---P}$), the dormant specie, and the radical concentration is controlled by the equilibrium established between active and dormant species [29, 44, 47, 48]. These two CMRP mechanisms are illustrated in scheme 1.



Scheme 1. Degenerative transfer (DT) and reversible termination (RT) of CMRP reaction.

Besides the importance of the mechanism upon the control, the chosen cobalt complex plays an important role mediating the activation/deactivation equilibrium. We believe that the structures of metal complexes can be modified in different ways to achieve a better understanding over the functioning of the mediating systems and for development of more versatile and efficient controlling agents for CMRP. Here, in contrast to extensive research done with N_2O_2 tetradentate Schiff-base cobalt complexes as mediators in CMRP, we report the synthesis, characterization and X-ray structure of a series of NO bidentate Schiff base $\text{Co}(\text{II})$ complexes derived from different cycloalkylamines and their application on VAc polymerization via the CMRP mechanism.

2. Experimental

2.1. General remarks

All reagents were purchased from Aldrich Chemical Co. All reactions and manipulations were performed under a nitrogen atmosphere by using standard Schlenk techniques. Vinyl acetate (VAc) was washed with 5% NaOH solution, dried over anhydrous MgSO₄, and degassed by several freeze-thaw cycles before being distilled from CaH₂ and stored at -18 °C under nitrogen. CoCl₂ was dried in a reaction flask carefully under reduced pressure (0.5 torr) by heating with a hair dryer for 2 h immediately before use. Cyclopentylamine, cyclohexylamine, cycloheptylamine, salicylaldehyde, tetrabutylammonium hexafluorophosphate (*n*-Bu₄NPF₆) and 2,2'-Azobis(2-methylpropionitrile) solution (AIBN) (0.2 M in toluene) were used as acquired. Complexes **2b** and **2c** were prepared following the literature and their purity was checked by satisfactory elemental analysis and spectroscopic examination (FTIR and UV-Vis) [49, 50]. The synthesis and characterization of the ligands **1a-1c** and complexes **2a-2c** are reported in the Supporting Information.

2.2. Analyses

Elemental analyses were performed in a Perkin-Elmer CHN 2400 at Elemental Analysis Laboratory at Institute of Chemistry - USP. The FTIR spectra in KBr pellets were obtained on a Shimadzu IRAffinity-1 FT-IR spectrometer. ¹H and ¹³C{¹H} NMR spectra were obtained in CDCl₃ at 298 K on an Agilent MR 400 Ultrashield spectrometer operating at 400.13 and 100.61 MHz, respectively. The obtained chemical shifts were reported in ppm relative to the high frequency of TMS. Conversion was determined from the concentration of residual monomer measured by gas chromatography (GC) using a Shimadzu GC-2010 gas chromatograph equipped with flame ionization detector and a 30 m (0.53 mm I.D., 0.5 μm film thickness) SPB-1 Supelco fused silica capillary column. Anisole was added in polymerization and used as an internal standard. Analysis conditions: injector and detector temperature, 250 °C; temperature program, 40 °C (4 min), 20 °C/min until 200 °C, 200 °C (2 min). The molecular weights and the molecular weight distribution of the polymers were determined by gel permeation chromatography using a Shimadzu Prominence LC system equipped with a LC-20AD pump, a DGU-20A5 degasser, a CBM-20A communication modulo, a CTO-20A oven at 40 °C and a RID-10A detector, equipped with two Shimadzu columns (GPC-805: 30 cm, Ø =

8.0 mm). The retention time was calibrated with standard monodispersed polystyrene using HPLC-grade THF as an eluent at 40 °C with a flow rate of 1.0 mL/min. UV–vis measurements were performed on a Cary 400 UV–vis spectrophotometer (Varian) using 1 cm path length quartz cells. Toluene solutions of the complexes of 0.2 mmol L⁻¹ concentrations were used for these measurements.

2.3. Synthesis of ligands 1a-1c

To prepare the Schiff base ligands **1a-1c**, a solution of salicylaldehyde (4 mmol; 0.49 g) in methanol (20 mL) was slowly added over a solution of the appropriate amine (4 mmol; 0.34, 0.39 and 0.45 g for cyclopentylamine, cyclohexylamine and cycloheptylamine, respectively) in the same solvent (20 mL). The mixture was stirred at room temperature for 16 h and the product was obtained as a yellowish orange oil.

1a: Yield: 88%; Refractive index 1.5626; (a) UV–Vis: $\lambda_{\max(n)}$ (nm), $\epsilon_{\max(n)}$ [M⁻¹ cm⁻¹]: $\lambda_{\max(1)}$ (317), $\epsilon_{\max(1)}$ [5320]; (b) IR (KBr, cm⁻¹): ν C=N (1626), ν C–O (1277); (c) ¹H NMR (CDCl₃, 400 MHz): 13.68 (s, 1H, OH), 8.34 (s, 1H, CH=N), 7.28 (ddd, ³J_{b,a} = ³J_{b,c} = 7.5 Hz, ⁴J_{b,d} = 1.9 Hz, 1H, salicyl-ring), 7.23 (dd, ³J_{d,c} = 7.5 Hz, ⁴J_{d,b} = 1.9 Hz, 1H, salicyl-ring), 6.94 (dd, ³J_{a,b} = 7.5 Hz, ⁴J_{a,c} = 1.1 Hz, 1H, salicyl-ring), 6.86 (ddd, ³J_{c,d} = ³J_{c,b} = 7.5 Hz, ⁴J_{c,a} = 1.1 Hz, 1H, salicyl-ring), 3.75-3.82 (m, 1H, CH^{Pentyl}), 1.95-1.81 (m, 4H, CH₂^{Pentyl}), 1.65-1.76 (m, 4H, CH₂^{Pentyl}). ¹³C NMR (CDCl₃) δ 162.3, 161.3, 131.8, 130.9, 118.4, 116.9, 70, 34.7, 24.5.

1b: Yield: 94%; Refractive index 1.5678; (a) UV–Vis: $\lambda_{\max(n)}$ (nm), $\epsilon_{\max(n)}$ [M⁻¹ cm⁻¹]: $\lambda_{\max(1)}$ (316,8), $\epsilon_{\max(1)}$ [7770]; (b) IR (KBr, cm⁻¹): ν C=N (1629), ν C–O (1274), (c) ¹H NMR (CDCl₃, 400 MHz): 13.82 (s, 1H, OH), 8.36 (s, 1H, CH=N), 7.28 (ddd, ³J_{b,c} = 7.5 Hz, ³J_{b,a} = 7.2 Hz, ⁴J_{b,d} = 1.9 Hz, 1H, salicyl-ring), 7.23 (dd, ³J_{d,c} = 7.5 Hz, ⁴J_{d,b} = 1.9 Hz, 1H, salicyl-ring), 6.94 (dd, ³J_{a,b} = 7.2 Hz, ⁴J_{a,c} = 1.1 Hz, 1H, salicyl-ring), 6.86 (ddd, ³J_{c,b} = ³J_{c,d} = 7.5 Hz, ⁴J_{c,a} = 1.1 Hz, 1H, salicyl-ring), 3.20-3.27 (m, 1H, CH^{Hexyl}), 1.78-1.86 (m, 4H, CH₂^{Hexyl}), 1.50-1.68 (m, 3H, CH₂^{Hexyl}), 1.43-1.25 (m, 3H, CH₂^{Hexyl}). ¹³C NMR (CDCl₃) δ 162.1, 161.4, 131.9, 131.1, 118.9, 118.3, 117.04, 77.3, 77.02, 76.7, 67.4, 25.5, 24.3.

1c: Yield: 91%; Refractive index 1.5652; (a) UV–Vis: $\lambda_{\max(n)}$ (nm), $\epsilon_{\max(n)}$ [M⁻¹ cm⁻¹]: $\lambda_{\max(1)}$ (316.2), $\epsilon_{\max(1)}$ [10000]; (b) IR (KBr, cm⁻¹): ν C=N (1630), ν C–O (1270); (c) ¹H NMR (CDCl₃, 400 MHz): 13.82 (s, 1H, OH), 8.36 (s, 1H, CH=N), 7.28 (ddd, ³J_{b,c} = 7.5 Hz, ³J_{b,a} =

7.2 Hz, $^4J_{b,d} = 1.9$ Hz, 1H, salicyl-ring), 7.23 (dd, $^3J_{d,c} = 7.5$ Hz, $^4J_{d,b} = 1.9$ Hz, 1H, salicyl-ring), 6.94 (dd, $^3J_{a,b} = 7.5$ Hz, $^4J_{a,c} = 1.1$ Hz, 1H, salicyl-ring), 6.86 (ddd, $^3J_{c,b} = ^3J_{c,d} = 7.5$ Hz, $^4J_{c,a} = 1.1$ Hz, 1H, salicyl-ring), 3.37-3.46 (m, 1H, CH^{Heptyl}), 1.74-1.85 (m, 4H, CH₂^{Heptyl}), 1.50-1.68 (m, 8H, CH₂^{Heptyl}). ¹³C NMR (CDCl₃) δ 161.66, 161.39, 131.92, 131.02, 118.91, 118.29, 116.99, 77.34, 77.08, 76.83, 70.12, 36.40, 28.54, 24.24.

2.4. Crystal structure determination

Red crystals of **2a** and **2b** were grown by slow evaporation from a MeOH solution at room temperature. The data collections were performed using Mo-K α radiation ($\lambda = 71.073$ pm) on a BRUKER APEX II Duo diffractometer. Standard procedures were applied for data reduction and absorption correction [51]. The structure was solved with SHELXS97 using direct methods [52] and all non-hydrogen atoms were refined with anisotropic displacement parameters with SHELXL2014 [52]. Hydrogens were placed at idealized positions using the riding model option of SHELXL2014 [52]. The absolute structure showed a flack parameter value of 0.011(17) and was refined as a 2-component inversion twin. More details on data collections and structure determination are in table 1.

2.5. Theoretical calculations

The structures of the compounds under study were optimized using the density functional theory (DFT) at the level of the hybrid functional PBE0 [53], implemented in Gaussian 09 [54], using the TZVP triple-zeta basis set [55]. The optimizations and calculation of the vibrational frequencies were done without any symmetry constraints. As the Co(II) complexes under study are high-spin pseudotetrahedral compounds ($S = 3/2$) [56, 57], all calculations were done considering a multiplicity equal to 4. After optimization, in all cases, $\langle S^2 \rangle = S(S+1) = 3.75$, suggesting the desirable non-existence of spin contamination in the generated orbital-based wave functions. For the Co(III) complexes formed by the coupling between the Co(II) complex and the vinyl acetate radical, the multiplicity was defined as being unitary. There are several previous studies which have reported DFT calculations of CMRP dormant species models [22, 58-67]. Here, in order to reproduce the experimental conditions, the simulations involving these compounds were also done under condition of solvation. For this, the previous structure was reoptimized using the model IEFPCM [68] to build a dielectric continuum with the

characteristics of dichloromethane, in a self-consistent reaction field procedure [54]. The structure of the product of coupling between the Co(II) complexes and the vinyl acetate radical was optimized only under solvation condition. The electronic spectra were calculated for the first sixty electronic states also considering the molecules solvated in dichloromethane (IEFPCM), using the same DFT functional and basis set previously described.

2.6. CMRP procedure

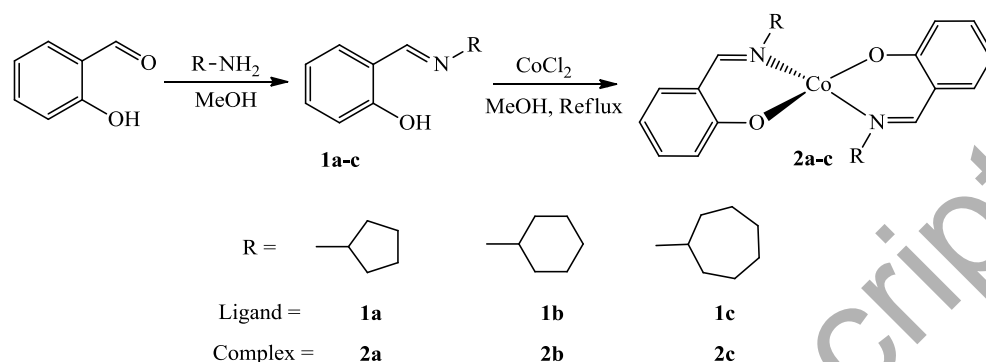
In a typical CMRP experiment, 0.02 mmol of Schiff base Co(II) complex (8.7, 9.3 and 9.8 mg for **2a**, **2b** and **2c**, respectively) and 0.065 mmol of AIBN (10 mg) were placed in a 50 mL Schlenk flask and degassed by three vacuum/nitrogen cycles. Dry, degassed vinyl acetate (5 mL, 54 mmol) was then added using a syringe under nitrogen. The red mixture was stirred and heated at 65 °C to start the polymerization. Samples were withdrawn at different reaction times and analyzed by GC to determine monomer conversion and by SEC-THF for molecular parameters using PS calibration, after addition of TEMPO to neutralize radicals.

3. Results and discussion

3.1. Synthesis and Characterization

The Schiff bases were prepared in high yields by condensation of salicylaldehyde with stoichiometric amounts of the desired amine in methanol; the corresponding products (**1a-1c**) were obtained under mild conditions (scheme 2). Confirmation of these products was demonstrated by spectroscopic methods. The azomethine proton ($CH=N$) resonance is observed within the range of 8.3–8.4 ppm for *N*-cycloalkyl salicylaldimines (**1a-1c**), as the electron-withdrawing phenyl group de-shields the azomethine proton and shifts the resonance to relatively low field (figure S1 and table S1). The $CH=N$ resonance appears as a broad singlet for all compounds in $CDCl_3$, providing further evidence that in solution these compounds exist mainly in the enol-imino tautomeric form. In all cases, a singlet for OH has a distinct down-field resonance at 13.8 ppm, characteristic for the acidic proton involved in a strong intramolecular hydrogen bond [69]. All cobalt(II) Schiff base complexes (**2a-2c**) were successfully synthesized in good yields in a single step from the metallation of the corresponding ligands with $CoCl_2$ under mild conditions by stirring under reflux (scheme 2) and were characterized by FTIR and UV-Vis spectroscopy (see discussion in the SI), elemental analysis, cyclic voltammetry and two

of the complexes were further studied by single crystal X-ray crystallography. Additional characterizations of **2a** and **2b** were necessary to complete the early presented studies [49, 50], to better understand their reactivity in the current purpose.



Scheme 2. Synthesis of ON donor Schiff bases **1a-c** and their cobalt(II) complexes **2a-c**.

The X-ray structure analysis of **2a** and **2b** confirmed the spectroscopic data. The crystal data and refinement details are listed in table 1. The compounds crystallized as discrete, neutral molecules in the non-centrosymmetric space group *Cc* and centrosymmetric space group *P2₁/c* for **2a** and **2b**, respectively. Figure 1 illustrates ellipsoid representation for one of the molecules in the asymmetric unit of **2a** as a representative of the cobalt(II) complexes. The asymmetric unit containing two molecules of **2a** as well as the molecular structure of **2b** are given in figures S2 and S3, respectively. Selected bond lengths and angles are presented in table 2. Both molecules contained in the asymmetric unit of **2a** present considerable disorder with 51.6 and 60.6 percent occupations for major components of the cyclopentyl group of one of the ligands. Attempts on the acquisition of better quality crystals of **2a** were not successful, however, good R values were obtained. Each ligand is deprotonated and coordinates to Co(II) ion via the phenolate and imine donor atoms in the usual *trans* configuration in which the cobalt(II) ion is tetracoordinated arranged in a tetrahedral geometry. Bond angles in **2a-b** confirm the tetrahedral geometry around the cobalt atom, with the N(1)–Co–N(2) (116.62(16)/123.08(17)° for **2a** and 118.15(6)° for **2b**) and O(1)–Co–O(2) angles (111.66(17)/116.60(16)° for **2a** and 120.93(7)° for **2b**). The C–O (1.297(6)–1.313(2) Å) and C–N bonds (1.281(2)–1.289(2) Å) are within the ranges between carbon–oxygen and carbon–nitrogen single and double bonds. This reflects a considerable delocalization of π -electron density within the six-membered rings.

The theoretical geometric parameters (bond lengths and angles) in table 2 show good agreement with the measured data in X-ray crystallography, despite some bond angles presenting an expressive discrepancy. This may be due to the fact that the theoretical data are related to a free molecule, whereas the experimental ones reflect intermolecular interactions in the crystalline reticulum. The solvation of the compound induces a minimal increase in these values.

3.2. Polymerization of VAc

To study the controlling ability of **2a-2c** on the VAc polymerization, the preliminary tests using each of the three complexes as controlling agent were investigated with AIBN as the initiator under the [VAc]/[AIBN]/[Co] molar ratio of 542/3.25/1 at 55 °C for 12 h. As is evident from the data presented in figure 2, the VAc polymerization mediated by **2a-2c** suggests that the level of control can be slightly tuned by the substitution of the cycloalkyl group on the Schiff base ligand. VAc polymerizations in the presence of **2a-2c**, the conversions increase from 35 to 75% with increasing CH₂ groups on the cycloalkyl ring from cyclopentyl up to cycloheptyl. The VAc polymerization mediated by **2a** and **2b** showed an induction period up to 2 h, which has been reported in CMRP [29, 31] and attributed to the time required to form the organocobalt(III) species in the medium. It proves that the polymerization mediated by **2a-b** must take place by degenerative transfer. Conversely, the absence of an induction time with **2c** suggests a reversible termination mechanism.

The linear semi-logarithmic plot of $\ln[\text{VAc}]_0/[\text{VAc}]_t$ versus time and the linear increase of molecular weight with conversion, in conjunction with moderate \bar{D} values, are consistent with a certain degree of control for the polymerization imparted by these complexes (figure 3). However, in repeated kinetic experiments, molecular weights were observed to be somewhat higher or lower than the theoretical values. The molecular weight distribution curves were monomodal throughout the polymerization (figure S4). This can be attributed to the number of growing radical chains being higher or lower than expected, resulting in an effective increase/decrease in the monomer concentration. All these results are consistent with a controlled polymerization, although the controllability is far from ideal when compared with that of reported for Co systems [23-30].

As the substituents became more sterically hindered (from cyclopentyl to cycloheptyl), conversion increased. The increased steric hindrance around the Co center can explain this trend,

as it would create greater lability of the organo-cobalt bond and increase propagating radical concentrations. Greater deviations between theoretical and experimental values were obtained with the bulkier cycloheptyl substituent (complex **2c**), which ΔS were broader, indicating that this polymerization was not well controlled and suggesting that irreversible termination reactions were prevalent. Based on this, it is possible to infer that the difference in the reactivity of the complexes studied is directly related to the steric characteristics of the Schiff base ligands, which are modulated by their substituents (cycloalkyl groups).

A computational investigation was carried out to investigate the polymerization mechanism by mediators **2a-2c**. The theoretical simulations show that only one of the faces of the complexes is active to formation of R-Co(III) from Co(II) species. The high electron density at the side positioned by the oxygen atoms makes it not suitable for a coupling of the vinyl radical with the Co(II) center (figure 4a). The regions with intense red are those with the highest electronic density, which is in agreement with the distribution of Mulliken's charges (figure S5, table S3). On the other hand, the high spin density on the Co(II) at the opposite side, in addition to the lower electron density on the nitrogen atoms, tends to effectively direct the coupling (figure 4b and figure S6). In fact, all attempts done in the calculations to make the coupling between the vinyl radical and the Co(II) via the face with higher electronic density were unsuccessful. The estimated bond order of the Co(III)-C bond for these complexes varies between 0.53 and 0.54, values typical of single bonds, which characterizes the coordination between the monomer and the metal. For a DT mechanism, a second coupling of another propagating vinyl radical with a Co(III) center must occur for the formation of an intermediate six-coordinate complex R-Co(IV)-R. In all cases, the ΔG values are positive ($\Delta G = 1.4965$, 23.3013 and 65.9027 kJ mol⁻¹ for **2a**, **2b** and **2c**, respectively), but only for **2c**, both ΔG and ΔH values are positive ($\Delta H = -55.2326$, -47.0910 and 3.6862 kJ mol⁻¹ for **2a**, **2b** and **2c**, respectively), suggesting that formation of this intermediate complex is a rather disadvantageous process. Thus, the thermodynamic parameters explain the RT mechanism exerted by **2c**, whereas the polymerization mediated by **2a** and **2b** is associated with a DT mechanism.

4. Conclusion

The Schiff bases ligands **1a-1c** and their respective Co(II) complexes **2a-2c** were successfully synthesized. The Schiff base-Co(II) complexes **2a-2c** were characterized by FTIR, UV-Vis spectroscopy, elemental analysis, cyclic voltammetry, computational methods, and two of the complexes (**2a** and **2b**) were further studied by single crystal X-ray crystallography. The preliminary VAc polymerizations mediated by **2a-2c** as a function of time ($[VAc]/[AIBN]/[Co] = 542/3.25/1$ at 55 °C) were first order in monomer, as assessed by the linear dependence of $\ln([M]_0/[M]_t)$ versus time. The VAc polymerization mediated by **2a-2c** suggests that the level of control can be slightly tuned by the substitution of the cycloalkyl group on the Schiff base ligand. The difference in the reactivity of the complexes studied was related to the steric characteristics of the Schiff base ligands, which are modulated by their substituents (cycloalkyl groups). The thermodynamic parameters explain the RT mechanism exerted by **2c**, while the polymerization mediated by **2a** and **2b** is associated with a DT mechanism.

Supplementary data

CCDC 1817953 contain the supplementary crystallographic data for **2a**. These data can be obtained free of charge via <http://www.ccdc.cam.ac.uk/conts/retrieving.html>, or from the Cambridge Crystallographic Data Centre, 12 Union Road, Cambridge CB2 1EZ, UK; Fax: (+44) 1223 336 033; or E-mail: deposit@ccdc.cam.ac.uk.

Acknowledgements

The authors are indebted to the financial support from FAPESP (Proc. 2013/11883-0 and 2013/10002-0), FAPEMIG (APQ 00583-13 and 03017-16) and CNPq (307443/2015-9). The authors also acknowledge the Instituto de Química de São Carlos/USP-Brazil for the NMR spectra acquisition.

References

- [1] P.G. Lacroix. *Eur. J. Inorg. Chem.*, 339 (2001).
- [2] M.J. O'Donnell. *Acc. Chem. Res.*, **37**, 506 (2004).
- [3] E. Hadjoudis, I.M. Mavridis. *Chem. Soc. Rev.*, **33**, 579 (2004).
- [4] K.C. Gupta, A.K. Sutar. *Coord. Chem. Rev.*, **252**, 1420 (2008).
- [5] M. Andruh. *Chem. Commun.*, **47**, 3025 (2011).
- [6] H. Miyasaka, A. Saitoh, S. Abe. *Coord. Chem. Rev.*, **251**, 2622 (2007).
- [7] I.P. Oliveri, S. Failla, G. Malandrino, S. Di Bella. *New J. Chem.*, **35**, 2826 (2011).
- [8] Y.B. Cai, J. Zhan, Y. Hai, J.L. Zhang. *Chem. Eur. J.*, **18**, 4242 (2012).
- [9] G. Consiglio, S. Failla, P. Finocchiaro, I.P. Oliveri, S. Di Bella. *Dalton Trans.*, **41**, 387 (2012).
- [10] L. Zhou, Y. Feng, J.H. Cheng, N. Sun, X.G. Zhou, H.F. Xiang. *RSC Adv.*, **2**, 10529 (2012).
- [11] S.M. Borisov, R. Saf, R. Fischer, I. Klimant. *Inorg. Chem.*, **52**, 1206 (2013).
- [12] L. Canali, D.C. Sherrington. *Chem. Soc. Rev.*, **28**, 85 (1999).
- [13] D.A. Atwood, M.J. Harvey. *Chem. Rev.*, **101**, 37 (2001).
- [14] P.G. Cozzi. *Chem. Soc. Rev.*, **33**, 410 (2004).
- [15] R. Drozdak, B. Allaert, N. Ledoux, I. Dragutan, V. Dragutan, F. Verpoort. *Adv. Synth. Catal.*, **347**, 1721 (2005).
- [16] Z. Li, Z. Zheng, H. Cheng. *Tetrahedron: Asymmetry*, **11**, 1157 (2000).
- [17] R.M. Wang, C.J. Hao, Y.F. He, Y.P. Wang, C.G. Xia, *Polym. Adv. Technol.*, **13**, 6 (2002).
- [18] R.I. Kureshy, N.H. Khan, S.H.R. Abdi, S.T. Patel, R.V. Jasra. *Tetrahedron: Asymmetry*, **12**, 433 (2001).
- [19] V.G. Gibson, S.K. Spitzmesser. *Chem. Rev.*, **103**, 283 (2003).
- [20] A. Pärssinen, T. Luhtanen, M. Klinga, T. Pakkanen, M. Leskelä, T. Repo. *Organometallics*, **26**, 3690 (2007).
- [21] S. Dutta, W.-C. Hung, B.-H. Huang, C.-C Lin. *Adv. Polym. Sci.*, **245**, 219 (2012).
- [22] A.N. Morin, C. Detrembleur, C. Jérôme, P.D. Tullio, R. Poli, A. Debuigne. *Macromolecules*, **46**, 4303 (2013).

- [23] C. Detrembleur, A. Debuigne, R. Bryaskova, B. Charleux, R. Jérôme. *Macromol. Rapid Commun.*, **27**, 37 (2006).
- [24] M. Hurtgen, A. Debuigne, C. Jérôme, C. Detrembleur. *Macromolecules*, **43**, 886 (2009).
- [25] A. Debuigne, R. Poli, C. Jérôme, R. Jérôme, C. Detrembleur. *Prog. Polym. Sci.*, **34**, 211 (2009).
- [26] B.B. Wayland, G. Poszmik, S.L. Mukerjee, M. Fryd. *J. Am. Chem. Soc.*, **116**, 7943 (1994).
- [27] L.D. Arvanitopoulos, M.P. Gruel, H.J. Harwood. *Polym. Prepr.*, **35**, 549 (1994).
- [28] L. Chiang, L.E.N. Allan, J. Alcantara, M.C.P. Wang, T. Storr, M.P. Shaver. *Dalton Trans.*, **43**, 4295 (2014).
- [29] C.M. Liao, C.C. Hsu, F.S. Wang, B.B. Wayland, C.-H. Peng. *Polym. Chem.*, **4**, 3098 (2013).
- [30] K.S. Santhosh Kumar, Y.Li, Y. Gnanou, U. Baisch, Y. Champouret, R. Poli, K.C. Robson, W.S. McNeil. *Chem. – Asian J.*, **4**, 1257 (2009).
- [31] A. Kermagoret, C. Jérôme, C. Detrembleur, A. Debuigne. *Eur. Polym. J.*, **62**, 312 (2015).
- [32] Z. Guan. *J. Am. Chem. Soc.*, **124**, 5616 (2002).
- [33] P.B.V. Scholten, J. Demarteau, S. Gennen, J. De Winter, B. Grignard, A. Debuigne, M.A.R. Meier, C. Detrembleur. *Macromolecules*, **51**, 3379 (2018).
- [34] M. Hurtgen, C. Detrembleur, C. Jérôme, A. Debuigne. *Polym. Rev.*, **51**, 188 (2011).
- [35] S. Yamago. *Chem. Rev.*, **109**, 5051 (2009).
- [36] J. Demarteau, B. Ameduri, V. Ladmiral, M.A. Mees, R. Hoogenboom, A. Debuigne, C. Detrembleur. *Macromolecules*, **50**, 3750 (2017).
- [37] A. Debuigne, J. Warnant, R. Jérôme, I. Voets, A. de Keizer, M.A.C. Stuart, C. Detrembleur. *Macromolecules*, **41**, 2353 (2008).
- [38] M.A. Semsarzadeh, A. Sabzevari. *J. Appl. Polym. Sci.*, **135**, 46057 (2018).
- [39] D. Cordella, F. Ouhib, A. Aqil, T. Defize, C. Jérôme, A. Serghei, E. Drockenmuller, K. Aissou, D. Taton, C. Detrembleur. *ACS Macro Lett.*, **6**, 121 (2017).
- [40] R. Poli. *Chem. Eur. J.*, **21**, 6988 (2015).
- [41] M.A. Semsarzadeh, P. Alamdari. *J. Polym. Res.*, **20**, 139 (2013).
- [42] Y. Zhao, M. Yu, S. Zhang, Z. Wu, Y. Liu, C.-H. Peng, X. Fu. *Chem. Sci.*, **6**, 2979 (2015).

- [43] A. Debuigne, R. Poli, C. Jérôme, R. Jérôme, C. Detrembleur. *Prog. Polym. Sci.*, **34**, 211 (2009).
- [44] C.-S. Hsu, T.-Y. Yang, C.-H Peng. *Polym. Chem.*, **5**, 3867 (2014).
- [45] B.B. Wayland, C.-H. Peng, X. Fu, Z. Lu, M. Fryd. *Macromolecules*, **39**, 8219 (2006).
- [46] A.E. Müller, D. Yan, G. Litvinenko, R. Zhuang, H. Dong. *Macromolecules*, **28**, 7335 (1995).
- [47] C.-H. Peng, J. Scricco, S. Li, M. Fryd, B.B. Wayland. *Macromolecules*, **41**, 2368 (2008).
- [48] C.-H. Peng, T.-Y. Yang, Y. Zhao, X. Fu. *Org. Biomol. Chem.*, **12**, 8580 (2014).
- [49] B.L. Sacconi, M. Ciampolini, F. Maggio, G.D. Re. *J. Am. Chem. Soc.*, **82**, 815 (1960).
- [50] I.A. Mustafa, M.H. Taki, T.K. Al-Allaf. *Asian J. Chem.*, **13**, 1039 (2001).
- [51] Bruker, *SAINT and SADABS*. Bruker AXS Inc., Madison, Wisconsin, USA (2012 and 2001).
- [52] G.M. Sheldrick, *SHELXS-97 and SHELXL2014, programs for the solution and refinement of crystal structures*, University of Göttingen, Göttingen, Germany (1997 and 2014).
- [53] C. Adamo, V. Barone. *J. Chem. Phys.*, **13**, 6158 (1999).
- [54] G09: Gaussian 09, Revision E.01. M.J. Frisch, G.W. Trucks, H.B. Schlegel, G.E. Scuseria, M.A. Robb, J.R. Cheeseman, G. Scalmani, V. Barone, B. Mennucci, G.A. Petersson, H. Nakatsuji, M. Caricato, X. Li, H. P. Hratchian, A.F. Izmaylov, J. Bloino, G. Zheng, J.L. Sonnenberg, M. Hada, M. Ehara, K. Toyota, R. Fukuda, J. Hasegawa, M. Ishida, T. Nakajima, Y. Honda, O. Kitao, H. Nakai, T. Vreven, J.A. Montgomery, Jr., J.E. Peralta, F. Ogliaro, M. Bearpark, J.J. Heyd, E. Brothers, K.N. Kudin, V.N. Staroverov, T. Keith, R. Kobayashi, J. Normand, K. Raghavachari, A. Rendell, J.C. Burant, S.S. Iyengar, J. Tomasi, M. Cossi, N. Rega, J.M. Millam, M. Klene, J.E. Knox, J.B. Cross, V. Bakken, C. Adamo, J. Jaramillo, R. Gomperts, R.E. Stratmann, O. Yazyev, A.J. Austin, R. Cammi, C. Pomelli, J. W. Ochterski, R. L. Martin, K. Morokuma, V.G. Zakrzewski, G.A. Voth, P. Salvador, J.J. Dannenberg, S. Dapprich, A.D. Daniels, O. Farkas, J.B. Foresman, J.V. Ortiz, J. Cioslowski, D. J. Fox, Gaussian, Inc., Wallingford, CT (2015).
- [55] A. Schaefer, C. Huber, R. Ahlrichs. *J. Chem. Phys.*, **100**, 5829 (1994).
- [56] M. Idešicová, J. Titiš, J. Krzystek, R. Boča. *Inorg. Chem.*, **52**, 9409 (2013).
- [57] M. Murrie. *Chem. Soc. Rev.*, **39**, 1986 (2010).

- [58] S. Maria, H. Kaneyoshi, K. Matyjaszewski, R. Poli. *Chem. Eur. J.*, **13**, 2480 (2007).
- [59] A. Debuigne, Y. Champouret, R. Jérôme, R. Poli, C. Detrembleur. *Chem. Eur. J.*, **14**, 4046 (2008).
- [60] A. Debuigne, C. Michaux, C. Jérôme, R. Jérôme, R. Poli, C. Detrembleur. *Chem. Eur. J.*, **14**, 7623 (2008).
- [61] S. Li, B. de Bruin, C.-H. Peng, M. Fryd, B.B. Wayland. *J. Am. Chem. Soc.*, **130**, 13373 (2008).
- [62] B. de Bruin, W.I. Dzik, S. Li, B.B. Wayland. *Chem. Eur. J.*, **15**, 4312 (2009).
- [63] A. Debuigne, R. Poli, R. Jérôme, C. Jérôme, C. Detrembleur. *ACS Symp. Ser.*, **1024**, 131 (2009).
- [64] A. Debuigne, R. Poli, J. De Winter, P. Laurent, P. Gerbaux, P. Dubois, J.-P. Wathelet, C. Jérôme, C. Detrembleur. *Chem. Eur. J.*, **16**, 1799 (2010).
- [65] A. Debuigne, R. Poli, J. De Winter, P. Laurent, P. Gerbaux, J.-P. Wathelet, C. Jérôme, C. Detrembleur. *Macromolecules*, **43**, 2801 (2010).
- [66] A. Debuigne, A.N. Morin, A. Kermagoret, Y. Piette, C. Detrembleur, C. Jérôme, R. Poli. *Chem. Eur. J.*, **18**, 12834 (2012).
- [67] Y. Piette, A. Debuigne, C. Jérôme, V. Bodart, R. Poli, C. Detrembleur. *Polym. Chem.*, **3**, 2880 (2012).
- [68] J. Tomasi, B. Mennucci, E. Cancès. *J. Mol. Struct. (Theochem)*, **464**, 211 (1999).
- [69] A. Karakas, A. Elmali, H. Unver, I. Svoboda. *J. Mol. Struct.*, **702**, 103 (2004).

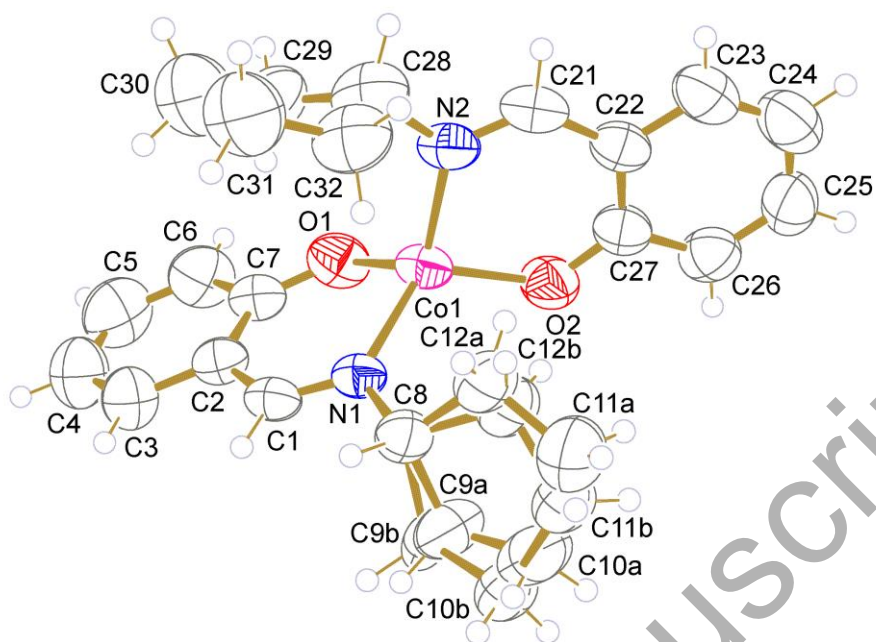


Figure 1. Thermal ellipsoid representation of **2a**. Only one of the two molecules in the asymmetric unit is shown. The cyclopentyl group of one of the ligands is disordered over two different sites (components labeled a and b). Hydrogens were omitted for clarity.

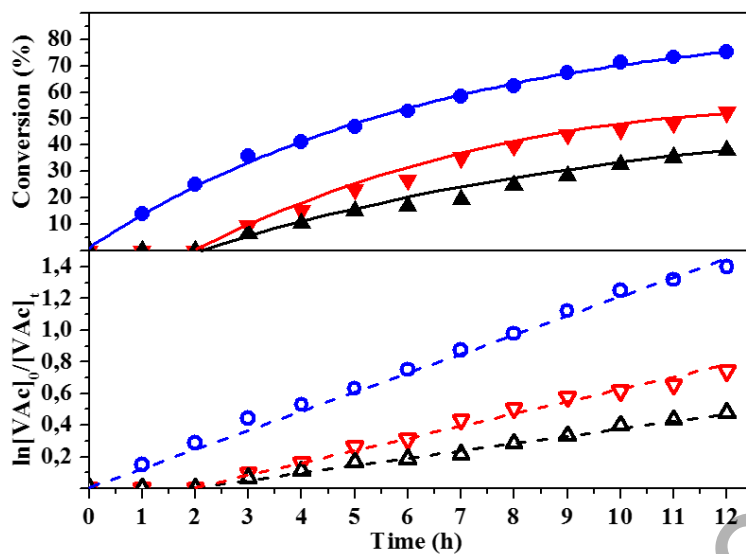


Figure 2. Dependence of conversion and $\ln([VAc]_0/[VAc]_t)$ on the reaction time for CMRP of VAc with **2a** (▲), **2b** (▼) and **2c** (●); $[VAc]/[AIBN]/[Co] = 542/3.25/1$ with 20 μmol of complex in bulk at 55 °C.

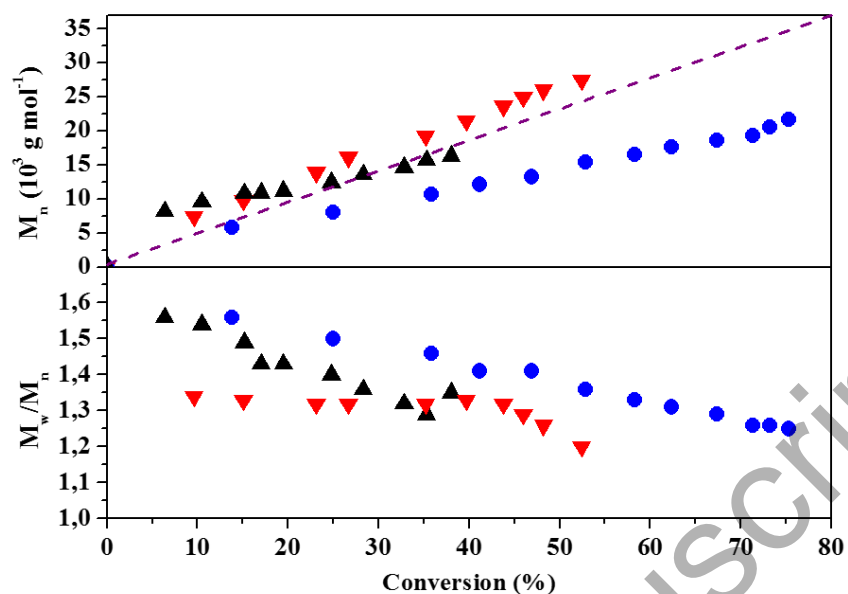


Figure 3. Dependence of M_n and M_w/M_n on the reaction time for CMRP of VAc with **2a** (\blacktriangle), **2b** (\blacktriangledown) and **2c** (\bullet); $[\text{VAc}]/[\text{AIBN}]/[\text{Co}] = 542/3.25/1$ with $20 \mu\text{mol}$ of complex in bulk at $55 \text{ }^\circ\text{C}$; $M_{n(\text{theor})}$ (dashed line).

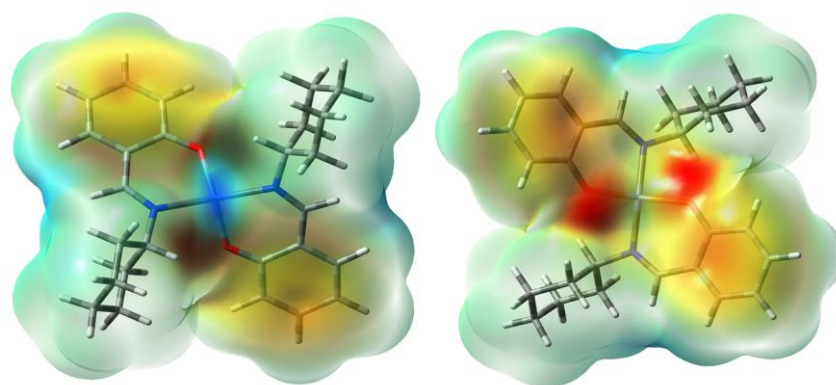


Figure 4. Electron density from total SCF density, mapped with the ESP: a) left - face susceptible to suffer coupling with the vinyl radical and b) right - face not susceptible to coupling.

Accepted Manuscript

Table 1. Crystal data and structure refinement for **2a** and **2b**.

	2a	2b
Empirical formula	C ₂₄ H ₂₈ CoN ₂ O ₂	C ₂₆ H ₃₂ CoN ₂ O ₂
Formula weight	435.41	463.46
Temperature (K)	296(2)	296(2)
Wavelength (Å)	0.71073	0.71073
Crystal system	Monoclinic	Monoclinic
Space group	<i>Cc</i> *	<i>P2₁/c</i>
<i>a</i> (Å)	12.3519(3)	21.8053(13)
<i>b</i> (Å)	44.7869(12)	10.0973(5)
<i>c</i> (Å)	8.9883(2)	11.4065(6)
β (°)	118.1300(10)	105.16
<i>V</i> (Å ³)	4385.02(19)	2424.0(2)
<i>Z</i>	8	4
<i>D</i> _{calc} (g cm ⁻³)	1.319	1.270
Absorption coefficient (mm ⁻¹)	0.804	0.732
θ range for data collection (°)	1.819 to 26.452	1.935 to 26.465
Crystal size (mm ³)	0.500 × 0.140 × 0.070	0.220 × 0.110 × 0.060
Number of reflections collected	29970	27486
Number of independent reflections/ <i>R</i> _{int}	7308 / 0.0288	4366 / 0.0592
Data / restraints / no. of parameters	7308 / 22 / 523	4366 / 0 / 280
Final <i>R</i> indices [<i>I</i> > 2σ(<i>I</i>)]	<i>R</i> ₁ = 0.0359, <i>wR</i> ₂ = 0.0894	<i>R</i> ₁ = 0.0351, <i>wR</i> ₂ = 0.0578
<i>R</i> indices (all data)	<i>R</i> ₁ = 0.0425, <i>wR</i> ₂ = 0.0933	<i>R</i> ₁ = 0.0691, <i>wR</i> ₂ = 0.0631
GOF	1.032	0.825
Largest difference peak and hole (eÅ ⁻³)	0.397 and -0.392	0.148 and -0.209

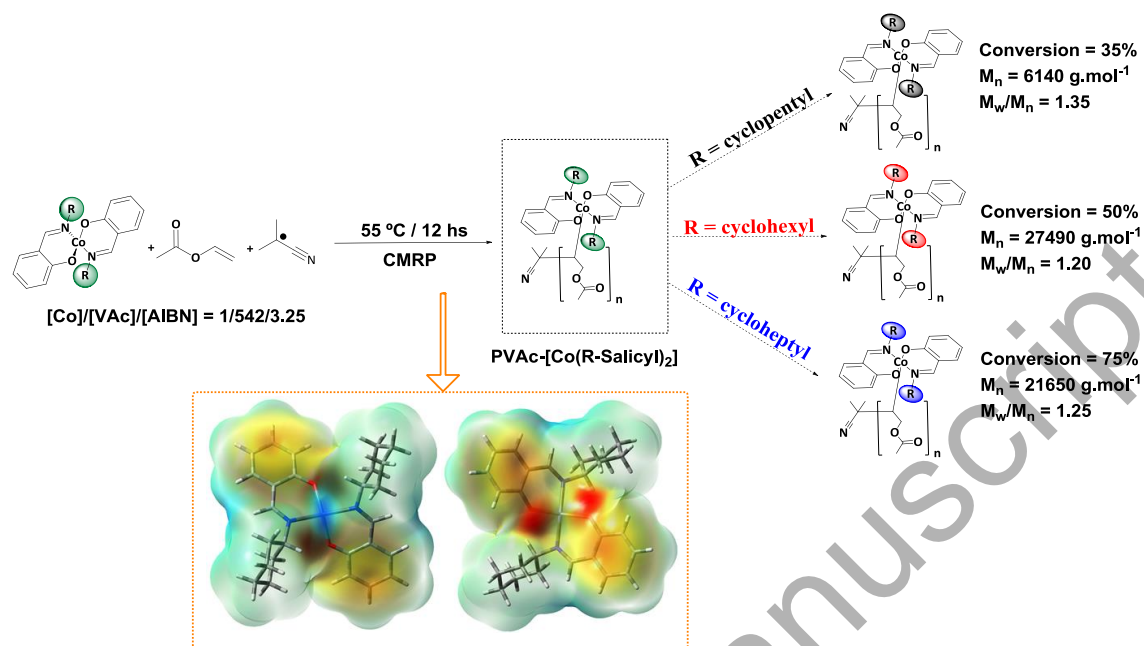
*Flack parameter: 0.011(17)

Table 2. Experimental and calculated selected bond lengths (Å) and angles (°) for **2a** and **2b**.

Geometric parameter	Complex 2a			Complex 2b		
	Experimental ^a	Theoretical (UPBE0) ^b	Discrepancy between the theoretical parameter for the isolated molecule and the experimental data (%)	Experimental	Theoretical (UPBE0) ^b	Discrepancy between the theoretical parameter for the isolated molecule and the experimental data (%)
N(1)-Co	1.996(3), 1.996(4)	2.052 (2.057)	+2.8, +2.8	1.9924(15)	2.044 (2.055)	+2.6
N(2)-Co	1.999(4), 1.988(3)	2.052 (2.057)	+2.6, +3.2	2.0018(15)	2.044 (2.055)	+2.1
O(1)-Co	1.907(3), 1.896(3)	1.922 (1.943)	+0.8, +1.4	1.8951(14)	1.926 (1.944)	+1.6
O(2)-Co	1.909(4), 1.904(3)	1.922 (1.943)	+0.7, +0.9	1.9182(14)	1.926 (1.944)	+0.4
N(1)-C(1)	1.286(6), 1.285(6)	1.283 (1.282)	-0.3, -0.2	1.289(2)	1.285 (1.284)	-0.3
N(2)-C(21)	1.283(6), 1.286(6)	1.283 (1.282)	0.0, -0.3	1.281(2)	1.285 (1.284)	+0.3
O(1)-C(7)	1.297(6), 1.302(6)	1.299 (1.300)	+0.1, -0.3	1.309(2)	1.298 (1.299)	-0.8
O(2)-C(27)	1.307(6), 1.308(5)	1.299 (1.300)	-0.7, -0.7	1.313(2)	1.298 (1.299)	-1.1
N(1)-Co-N(2)	116.62(16), 123.08(17)	157.62 (162.91)	+35.2, +28.1	118.15(6)	156.04 (160.64)	+32.1
O(1)-Co-O(2)	111.66(17), 116.60(16)	137.32 (128.04)	+23.0, +17.8	120.93(7)	137.96 (129.99)	+14.1
O(1)-Co-N(1)	95.87(15), 96.70(15)	92.38 (92.46)	-3.6, -4.5	96.17(6)	92.28 (92.09)	-4.0
O(2)-Co-N(1)	119.00(15), 114.76(15)	95.73 (95.01)	-19.6, -16.6	113.53(7)	96.27 (96.07)	-15.2
O(1)-Co-N(2)	118.65(17), 110.72(16)	95.73 (95.00)	-19.3, -13.5	113.50(6)	96.27 (96.06)	-15.2
O(2)-Co-N(2)	96.53(16), 96.36(14)	92.37 (92.46)	-4.3, -4.1	96.18(6)	92.28 (92.09)	-4.1
C(7)-O(1)-Co	125.1(3), 125.9(3)	128.87 (128.46)	+3, +2.3	125.15(13)	128.90 (128.62)	+3.5
C(27)-O(2)-Co	125.6(3), 125.7(3)	128.87 (128.45)	+2.6, +2.5	124.58(13)	128.89 (128.62)	+3.5
C(1)-N(1)-Co	119.9(3), 119.7(3)	123.09 (123.13)	+2.6, +2.8	120.11(14)	123.27 (123.41)	+2.6
C(21)-N(2)-Co	120.5(3), 119.8(3)	123.09 (123.13)	-0.6, +2.7	120.41(13)	123.27 (123.41)	+2.4

^a Values for two crystallographically independent molecules; ^b isolated molecule (in parenthesis, values for the solvated compound)

Graphical Abstract



Accepted Manuscript